Journal of the European Ceramic Society **13** (1994) 419–426

Reaction Sintering of Aluminium Titanate: II—Effect of Different Alumina Powders

V. Buscaglia,[a] P. Nanni,[b] G. Battilana,[a] G. Aliprandi[c] & C. Carry[d]

[a] Istituto di Chimica Fisica Applicata dei Materiali, C. N. R., via De Marini 6, 16149 Genoa, Italy
[b] Istituto di Chimica, Università di Genova, Fiera del Mare, Piazzale Kennedy, 16129 Genoa, Italy
[c] Istituto di Scienza e Tecnologia per l'Ingegneria Chimica, Viale Causa, 16145 Genoa, Italy
[d] Ecole Polytechnique Fédérale de Lausanne, Departement des Matériaux, MX-D Ecublens, 1015 Lausanne, Switzerland

(Received 29 December 1992; revised version received 5 May 1993; accepted 4 December 1993)

Abstract

Reaction sintering of aluminium titanate was studied starting from different commercial alumina powders and rutile. The formation of titanate, the successive sintering process and the corresponding microstructure evolution have been investigated using differential dilatometry, X-ray powder diffraction and scanning electron microscopy. Reaction sintering of pure Al_2TiO_5 results in a coarse-grained material with low density; the dependence of the average grain size of the resulting material from the level of impurities of the starting alumina is qualitatively discussed; the purest aluminas result in the largest grains. Addition of 2 wt% of MgO changes the mechanism of titanate formation, resulting in a strong reduction of the average grain size and remarkable influence on densification of the final material. Since final microstructure is mainly determined by the amount of MgO added, the influence of the nature of alumina powder is less pronounced in comparison with pure Al_2TiO_5.

Das reaktive Sintern von Aluminiumtitanat wurde, ausgehend von verschiedenen kommerziellen Aluminiumoxyd- und Rutilpulvern, untersucht. Die Bildung von Titanat, der fortschreitende Sinterprozeß und das sich ergebende Mikrogefüge wurde mit Hilfe von Differentialdilatometrie, Röntgenpulverbeugung und Rasterelektronenmikroskopie untersucht. Das reaktive Sintern von reinem Al_2TiO_5 ergibt ein grobkörniges Material mit geringer Dichte. Die Abhängigkeit der mittleren Korngröße des Endmaterials von den Verunreinigungen des Aluminiumoxyds wird qualitativ diskutiert; die reinsten Aluminiumoxyde ergeben die größten Körner. Die Zugabe von 2 Gew.% MgO verändert den Mechanismus der Titanatbildung und führt zu einer starken Abnahme der mittleren Korngröße und einer beträchtlichen Zunahme der Dichte des Endmaterials. Da das Mikrogefüge des Endmaterials hauptsächlich von der Menge des zugegebenen MgO bestimmt wird, ist der Einfluß des Aluminiumoxydpulvers weniger stark als bei reinem Al_2TiO_5.

On a étudié le frittage réactionnel du titanate d'aluminium à partir de rutile et de différentes poudres d'alumine, de qualité commerciale. La formation du titanate et l'évolution de la microstructure lors du frittage qui lui est consécutif ont été suivies par dilatométrie différentielle, diffraction X de poudres et microscopie à balayage. Le frittage réactionnel d'Al_2TiO_5 pur produit un matériau à gros grains et de faible densité; on discute qualitativement l'influence des concentrations en impuretés de l'alumine de départ sur la taille de grains du produit final; les poudres les plus pures conduisent à la plus grande taille de grains. L'ajout de 2% pond. de MgO modifie le mécanisme de formation du titanate, réduisant fortement la taille moyenne des grains et améliorant notablement la densité du produit final. La microstructure est alors determinée essentiellement par la quantité de MgO ajoutée, et la nature de la poudre d'alumine utilisée est moins cruciale que pour Al_2TiO_5 pur.

1 Introduction

Reaction sintering of aluminium titanate has been the subject of several studies, due to its very low expansion coefficient, low thermal conductivity and good thermal shock resistance.[1–8] This combination of properties makes it a candidate material, for many high-temperature structural applications, in particular as insulating material in internal combustion engines.[9] The mechanism of Al_2TiO_5 formation from the starting oxides Al_2O_3 and

Journal of the European Ceramic Society 0955-2219/94/$7.00

TiO_2 has been carefully investigated by Freudenberg[10] & Mocellin,[11,12] who have underlined the importance of the nucleation and growth process of the new phase in the development of the final microstructure in the temperature range 1280–1400°C. Aluminium titanate, nevertheless, is unstable below 1280°C[13] and decomposes to α-alumina and titania. It is known that some additives (MgO,[6] Fe_2O_3,[7] SiO_2,[5,6] ZrO_2[4–6]) are able to influence both the thermal stability and the microstructure of aluminium titanate, but the origin of such effects is not yet well understood. In Part I of this work,[14] the effect of MgO addition on the reactive sintering of aluminium titanate from α-Al_2O_3 and TiO_2 (rutile) was investigated. The presence of MgO changes the mechanism of titanate formation, making easy the nucleation of the new phase through the intermediate formation of $MgAl_2O_4$ followed by the growth of Mg-rich titanate solid-solution particles. The main result is the dramatic reduction of the average grain size and a remarkable influence on the density of the final material. In the present study, Al_2TiO_5, and Al_2TiO_5 with 2 wt% MgO addition, were reaction sintered starting from different commercial aluminas and rutile. The aim of this work is to clarify possible effects of the properties of the starting alumina powders (purity, γ-phase contents, particle size...) on the formation reaction and sintering behaviour of the titanate and on the microstructure of the final material.

2 Experimental Procedure

The Al_2O_3 and TiO_2 powders used in this work are all commercially available. Nature, purity, chemical analysis and particle size are reported in Table 1. The Vaw alumina is a moderate-purity, low-cost powder for industrial applications. The Keramont alumina (100PCT/TLV/TWA) is a high-purity, high-cost monosized powder. The Criceram alumina (Exal Al5Z) is produced using the Exal process. The original Aluminia alumina consisted of a coarser powder ('sandy' alumina) which has been ground in a zirconia mill to reduce the particles size. For the sake of brevity, the different sets of specimens will be indicated as follows: V (Vaw), K (Keramont), E (Criceram Exal) and S (Aluminia 'sandy') when prepared from Al_2O_3 and TiO_2, whereas VM, KM, EM and SM are the corresponding ones prepared with MgO addition. The preparation of the greens and the sintering conditions have been described previously.[14] The reactive and densification behaviour of the different materials was studied up to 1600°C with a heating rate of 1°C/min, using differential dilatometry.[14] The specimens obtained after sintering were characterized for their physical and microstructural properties. The phases present were determined by X-ray diffraction (Philips PW1050/PW1729/PW1710). The density was measured by a water-immersion method, coating the specimens with a thin sprayed Teflon layer to avoid water absorption. The density of the green samples was determined by geometry and weight. Microstructure was observed by SEM (Philips 515), after infiltration of the specimens in epoxy resin and metallographic preparation. The average grain size of Al_2TiO_5 was evaluated through the intercept method on the basis of five SEM images, corresponding to about 250 intercepted grains, and expressed as mean intercept length.

Table 1. Characteristics of the starting powders

	TiO_2	Al_2O_3			
Origin	Aldrich	Vaw	Keramont	Criceram	Aluminia
Purity (%)	99·9	99	99·99	99·99	99
Phase	Rutile	α	α	α	γ
Size (μm)	X_{50}=1	X_{50}=0·8	X_{50}=0·5	X_{50}=0·3	≤5
Na		3000	30	40	2500
Fe		600	40	25	900
Si		500	100	40	
Mg		800	20		

3 Results

3.1 Densification

The density (g/cm^3) and the densification rate (g/(cm^3 min)) versus temperature for pure Al_2TiO_5 specimens are presented in Fig. 1(a)–(c) (the theoretical density of Al_2TiO_5 is 3·7 g/cm^3). The densification curves of the K specimen have already been reported in Fig. 1(a) of Ref. 14. The overall process of reaction sintering consists of three different stages:

(i) Sintering of the starting oxides mixture (first contraction);
(ii) formation of Al_2TiO_5 (intermediate expansion);
(iii) sintering of Al_2TiO_5 (second contraction, lacking on V specimen).

The sintering of the Al_2O_3/TiO_2 matrix starts at 1000–1100°C and stops at 40–70°C above the reported formation temperature of Al_2TiO_5 (1280°C[13]), corresponding to the maximum of the density curve. The position of this maximum corresponds to the temperature at which the expansion related to Al_2TiO_5 formation offsets the matrix densification. In all cases, with less evidence for the V series, the densification rate curve

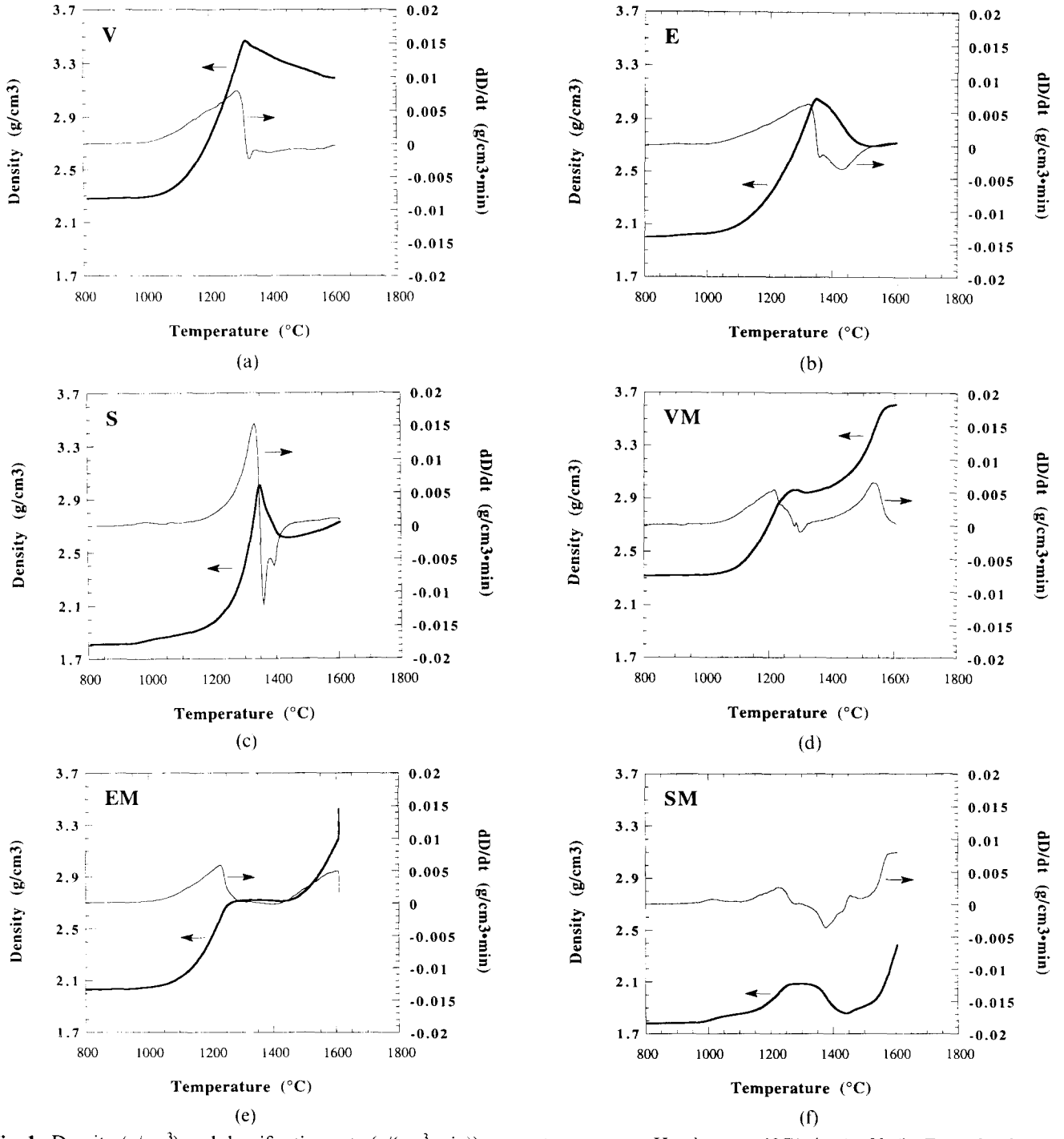

Fig. 1. Density (g/cm^3) and densification rate (g/(cm^3 min)) versus temperature. Heating rate 1°C/min. (a) V; (b) E; (c) S; (d) VM; (e) EM; (f) SM.

exhibits two minima, confirming the previous result obtained for K specimens[14] and indicating the presence of two different reaction mechanisms. Specimens with MgO addition present a different densification behaviour. These differences can be observed on the density curves of Fig. 1(d)–(f). The principal features of VM and EM specimens are similar to those observed for densification of the KM specimens which has been already reported in Fig. 1(b) of Ref. 14. In particular:

—The titanate formation temperature is lowered by the formation of the solid solution; as a consequence the densification of the matrix is reduced;

—the stage of expansion is reduced or eliminated (KM), due to the less sharp formation rate of the titanate and to the densification of the titanate which starts at ≈1300°C;

—the densification rate in the range 1450–1600°C is much higher than that of the corresponding specimens without MgO; in particular for VM specimens the behaviour is even inverted from expansion to shrinkage.

The SM specimens, in contrast, undergo a considerable expansion, with three minima of the densification rate and show a poor densification of the starting oxides in comparison with the other series. To summarize the sintering behaviour of

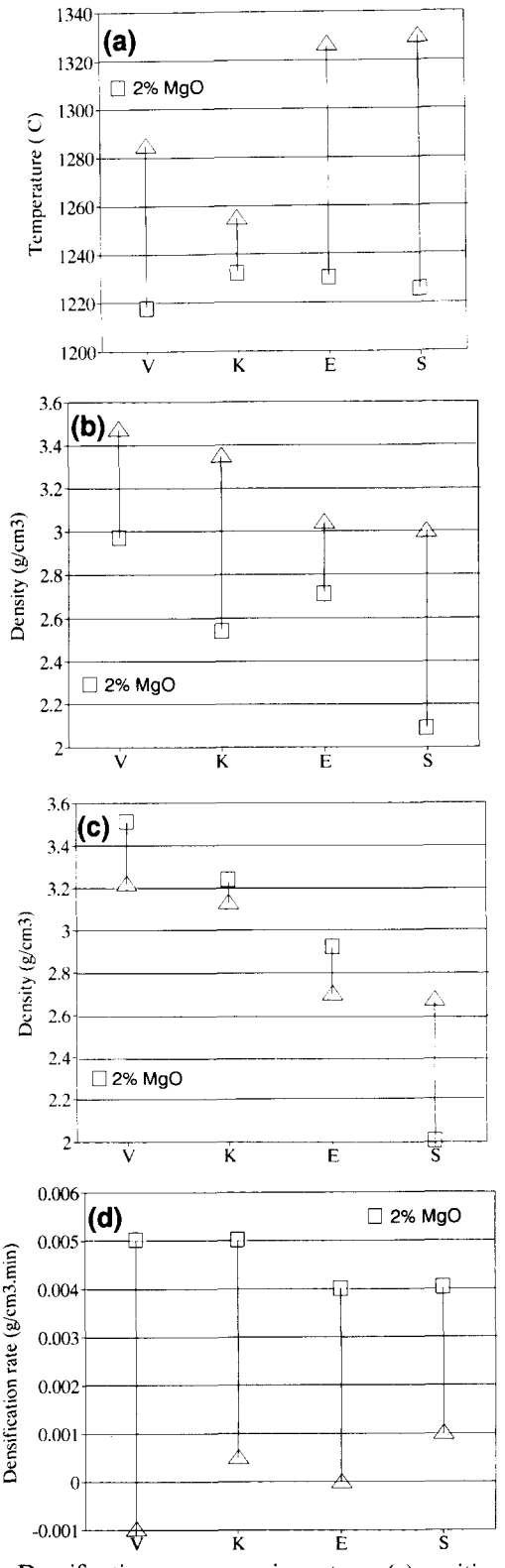

Fig. 2. Densification versus specimen type: (a) position of the maximum of the densification rate curve (°C); (b) value of the maximum of the density curve (g/cm^3); (c) density at 1550°C (g/cm^3); (d) densification rate at 1550°C (g/(cm^3 min)).

the different specimens, the values of four parameters taken from the density curves have been plotted in Fig. 2 (a)–(d): (a) the temperature of the first maximum of the densification rate (which can be approximated to the formation temperature of Al_2TiO_5); (b) the value corresponding to the maximum of the density curve (for KM specimens the density corresponding to the minimum

Table 2. Relative density of green samples and specimens sintered at 1450 and 1550°C for 6, 12 and 24 h

Sintering time (h)	*V*	*VM*	*K*	*KM*	*E*	*EM*	*S*	*SM*
T=1450°C								
Green	61·6	62·7	51·7	52·4	54·3	54·9	48·9	48·1
6	78·7	84·2	73·3	82·2	73·2	74·0	61·0	51·2
12	78·6	85·3	72·4	84·6	73·7	75·4	57·8	49·1
24	80·5	85·4	73·5	87·0	71·8	87·6	64·0	52·1
T=1550°C								
Green	61·6	62·7	51·7	52·4	54·3	54·9	48·9	48·1
6	78·6	93·1	73·9	92·2	69·4	79·8	66·4	58·3
12	81·4	91·3	74·4	91·7	71·0	82·0	66·9	58·0
24	82·1	91·5	75·8	93·1	71·2	84·7	65·3	58·0

of the densification rate); (c) the density, and (d) the densification rate at 1550°C. The higher densification rates result in a final larger contraction for KM, EM and VM series in comparison with the specimens without MgO. In spite of a densification rate close to that of EM, the density of SM specimens at 1550°C is much lower, as a consequence of the lowest green density and the lowest initial densification. Other dilatometer runs, performed up to 1700°C on the SM system, have shown a maximum shrinkage rate at ≈1650°C and a shrinkage at 1700°C of about 19%, with a strong increase in density. The final relative percentage density of the specimens sintered at 1450 and 1550°C for 6, 12 and 24 h, with and without MgO addition, is presented in Table 2. For the sake of comparison, the green density is also reported: a strong dependence on the nature of the alumina powder can be observed. In particular, V alumina gives the densest green samples (≈2·3 g/cm^3) and S alumina the least dense (≈1·8 g/cm^3). The main reason of the poor initial density of S specimens is related to the formation of quite porous aggregates of Al_2O_3 (≈5–10 μm) during the mixing process. The addition of MgO has little influence on the green density. The data confirm the results from dilatometry. After sintering the densification scale is V > K > E > S, independent of temperature and sintering time. The K green samples, less dense than those of E specimens, result in denser sintered materials. For V, K and E specimens there is little effect on raising the sintering temperature from 1450 to 1550°C, whereas for S specimens there is ≈10% densification increase. MgO has a strong influence on densification, in particular at 1550°C. For VM, KM and EM specimens there is a remarkable increase of the final density: from 79 to 93% for VM, from 74 to 92% for KM and from 69 to 80% for EM after 6 h sintering. The most beneficial effect is for the KM series. For S specimens, in contrast, MgO has the opposite effect, reducing density. In particular, at 1450°C, the final density is almost the same as the green density.

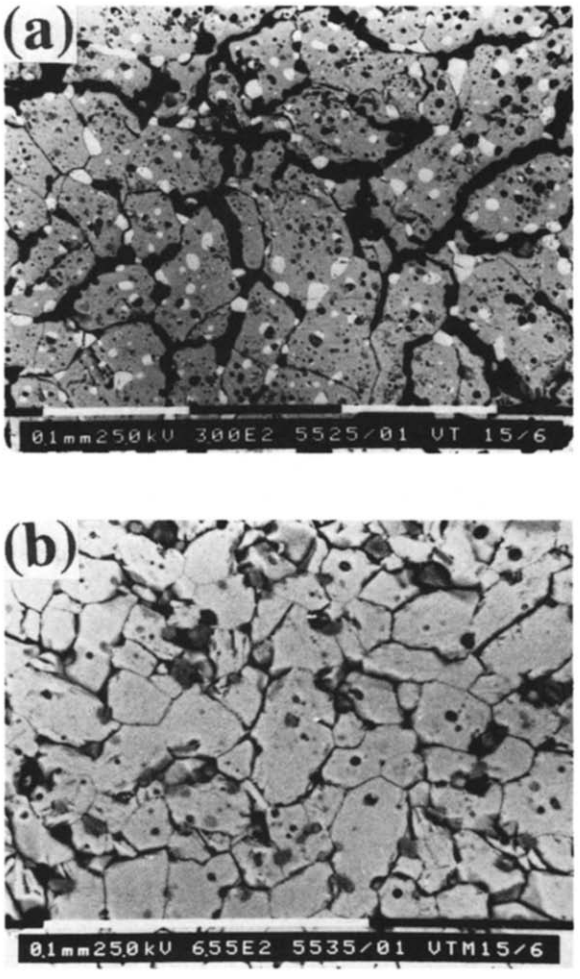

Fig. 3. Microstructure (BEI image) of (a) V and (b) VM specimen after 6 h sintering at 1550°C.

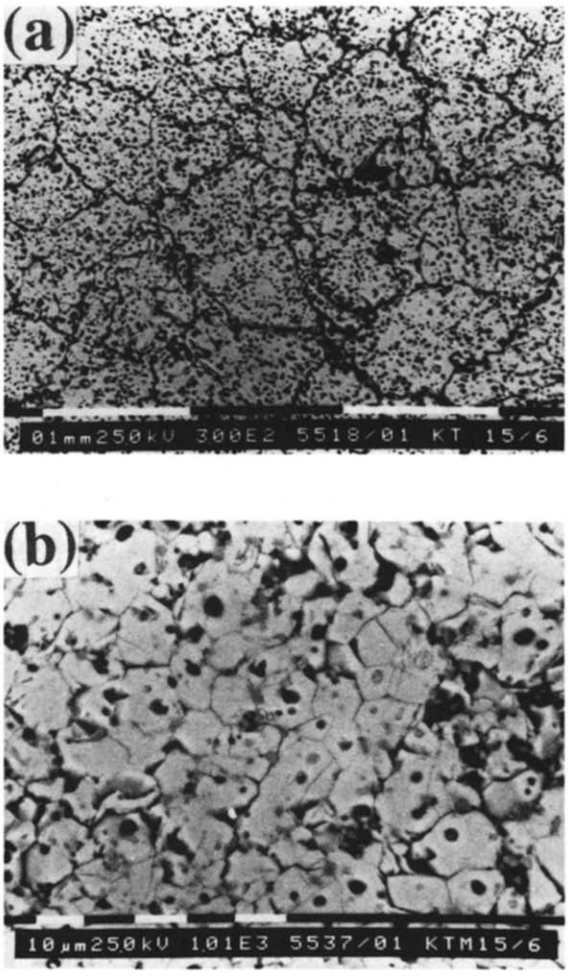

Fig. 4. Microstructure (BEI image) of (a) K and (b) KM specimen after 6 h sintering at 1550°C.

3.2 Microstructure

Since reaction sintering in the presence of MgO has always been carried out starting from an equimolar Al_2O_3–TiO_2 mixture, and the formation of the solid solutions occurs by substitution of 2 Al^{3+} by 1 Mg^{2+} and 1 Ti^{4+},[6] the specimens with MgO addition lead to the formation of $Al_{2(1-x)}Mg_xTi_{(1+x)}O_5$, with x = 0·099 (theoretical) and contain an excess of Al_2O_3 (9·89 wt%), which forms a second phase in the sintered materials. The calculation of x from the titanate cell constant determined by X-ray diffraction gives results in good agreement with the expected values, confirming that Mg enters completely into the solid solution. The values of the average grain size and the corresponding standard deviation for specimens sintered for 6, 12 and 24 h at 1550°C are reported in Table 3. The E, EM, S and SM series, due to their higher porosity, are observed with some difficulty and only the value for 6 h treatment is reported. Considering the uncertainty of the measurement, grain growth is noticeable for the VM series only. After sintering, the V specimens present grains with inclusions of unreacted TiO_2 (white) and Al_2O_3 (dark grey), beside pores of spherical shape (black) (Fig. 3(a)). Often TiO_2 particles are present at grain boundaries and large voids exist between the titanate grains. MgO addition results in much smaller grains and in a reduction of the total porosity; the specimens appear well sintered (Fig. 3(b)). The dark particles consist of Al_2O_3 and are often located at three-grain joints and are related to the excess of alumina in the starting mixtures, as already mentioned. The K specimens appear completely reacted, with the formation of large grains with extensive internal porosity (Fig. 4(a)). The large intergranular voids, typical of V specimens, are absent. MgO addition results in even smaller grains in comparison with the VM specimens (Fig. 4(b)). The residual Al_2O_3 particles are also of

Table 3. Average grain size (mean intercept length) for specimens sintered at 1550°C for 6, 12 and 24 h

Sintering time (h)	*V*	*VM*	*K*	*KM*	*E*	*EM*	*S*	*SM*
6	100±7	20±2	200±28	14±2	396±20	17±2	8	5
12	110±7	29±4	205±21	11±2	—	—	—	—
24	109±10	28±2	194±27	13±1	—	—	—	—

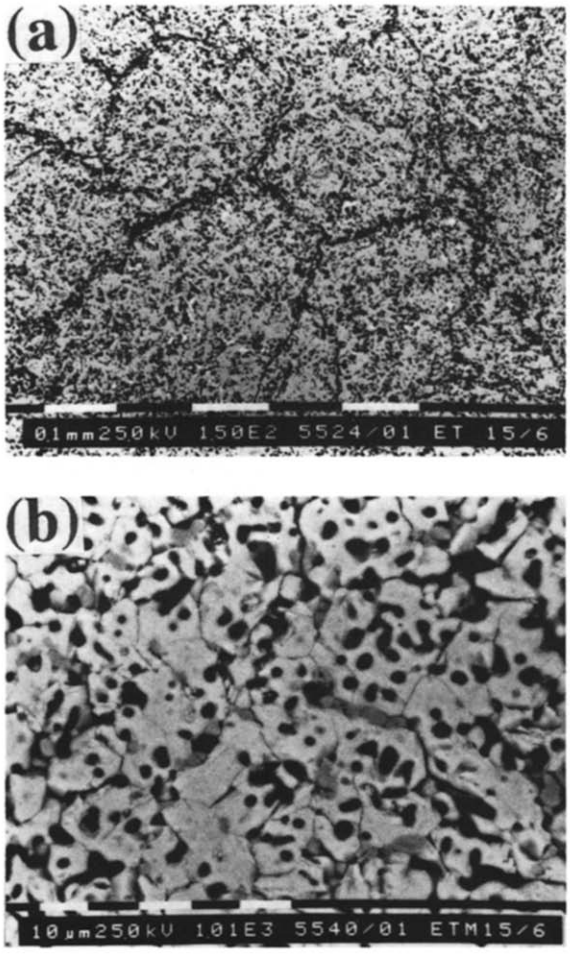

Fig. 5. Microstructure (BEI image) of (a) E and (b) EM specimen after 6 h sintering at 1550°C.

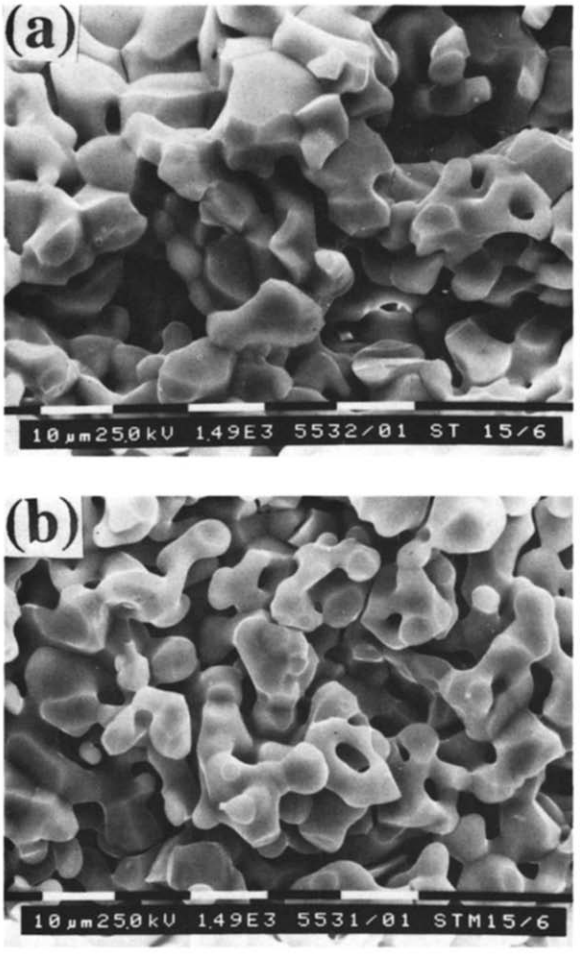

Fig. 6. Fractographs (SEI image) of (a) S and (b) SM specimen after 6 h sintering at 1550°C.

reduced size. The E specimens are similar to the K series, with formation of very large grains presenting extensive internal porosity and small particles of unreacted TiO_2 and Al_2O_3 (Fig. 5(a)). The EM specimens present a strong reduction of grain size, but a considerable residual porosity still remains (Fig. 5(b)), in agreement with the measured lower density: the EM specimens are only partially densified. S specimens are extremely porous and the resulting material is so fragile as to be crumbled by hand. A fractograph is presented in Fig. 6(a): no significant sintering is observed, in spite of the relatively reduced grain size. MgO addition reduces grain size, but increases porosity (Fig. 6(b)). The formation of bridges between particles can be observed, indicating the beginning of the sintering process. In conclusion, the microstructure of sintered specimens depends on the nature of the starting alumina powder and, as already underlined, it is strongly influenced by MgO addition. Specimens of pure Al_2TiO_5 develop large grains with extensive intra- and intergranular porosity; in contrast the formation of the solid solution results in a dramatic reduction of the grain size and a higher final density, with the exception of SM.

4 Discussion

The two minima of the densification rate curves for pure Al_2TiO_5 specimens correspond to two different overall reaction mechanisms as first reported by Freudenberg[10] & Mocellin[11,12] on the basis of isothermal reaction kinetics at different temperatures. The first minimum is located between 1335 and 1355°C and can be ascribed to the nucleation–growth process of titanate cells at a limited number of 'easy to nucleate' sites. The second minimum occurs around $\approx$1400°C ($\approx$1385 for K, $\approx$1395 for V, $\approx$1400 for S and $\approx$1430°C for E) and can be ascribed to the conversion of residual Al_2O_3 and TiO_2 particles by solid-state diffusion through Al_2TiO_5. The relative importance of the two stages depends on the nature of the starting alumina. K and S specimens are characterized by a rapid initial formation of Al_2TiO_5 and, as a consequence, a lower amount of unreacted oxide remains when the second, slower, formation stage starts. For this reason, the expansion process stops at relatively low temperature ($\approx$1410°C for K and $\approx$1440°C for S). From isothermal experiments carried out on the S series, the converted fractions are $\approx$60% at $\approx$1300°C,

90% at 1350°C and ≈ 100% at 1450°C after 30 min and the residual alumina is present in the α form.[15] The transformation from cubic γ- to hexagonal α-Al_2O_3 phase occurs between 1000 and 1200°C.[16] Hence, if the alumina is heated slowly, as in the present case, the phase change will be completed before the titanate formation temperature is reached and only a little influence on the reaction rate (the so-called Hedvall effect) is expected. V and E specimens, in contrast, have a much lower initial reaction rate and therefore a higher fraction of unreacted oxides still remains when the second stage starts. The expansion process stops at ≈ 1540°C for E and at temperatures >1600°C for V. For the latter, about 100 h at 1450°C are required for the complete conversion. The presence of Al_2O_3 and TiO_2 particles after 6 h sintering at 1550°C in E and, in particular, in V specimens confirms a slower conversion of the unreacted particles. The rate of the two kinetic stages is probably influenced by the microstructure developed in the oxide matrix during the heating stage before titanate formation. Observations carried out on V and S specimens after 3 h of isothermal treatment at 1250°C show coarsening of both TiO_2 and Al_2O_3, but a different microstructure. The initial accelerated densification has been explained in terms of both TiO_2 and Al_2O_3 transport through the rutile, due to the greater diffusion coefficient of Al ions in TiO_2 in comparison with Al ions in Al_2O_3.[10] The shrinkage values obtained from dilatometry, close to that of pure rutile, confirm this interpretation. The growth of the alumina grains is another important process which takes place in the matrix and can be described as Ostwald ripening of Al_2O_3 particles in a TiO_2 matrix.[10] Since the growth rate, for the same particle–matrix system, depends on the average radius of the particles,[17] alumina powders with initial different particle size and size distribution will result in different microstructure evolution, as effectively observed. Moreover, other factors like the formation of aggregates (mixing process), the surface structure of the powder (surface diffusion) and the level of impurities (doping effects) can influence the coarsening and sintering of TiO_2 and Al_2O_3 particles. The high growth rate of the titanate cells during the first reaction stage can be explained either by mass transport through bulk TiO_2 or along interfaces;[11] however, a pronounced influence of the microstructure is expected only for transport along interfaces. The conversion rate of the unreacted oxides particles trapped in the titanate cells (second kinetic stage) will be determined by their density and their size and, as a consequence, by the microstructure developed before reaction. For a fixed conversion value, the average Al_2O_3–TiO_2 distance will increase as the average particles radius increases and therefore the concentration gradient, responsible for mass transport, will decrease and the overall kinetics will slow down. This effect is particularly evident from the microstructure of V specimens; the continuous observed expansion is correlated to the slow conversion of the relatively big particles of TiO_2. Since densification and grain growth processes after titanate formation appear to be of limited importance, the average grain size of the final material is mainly determined by the density of 'easy to nucleate' available sites, which, in turn, is controlled by the level and the nature of the impurities. V and S specimens, prepared from less pure aluminas, present in fact a reduced grain size (in particular S) in comparison with K and E specimens. The initial rapid growth of the titanate grains can be inhibited by operating with higher heating rates, obtaining sintered material with smaller grains.[18] The final density is mainly determined by that achieved during the densification of the matrix; there is in fact a good correlation between the values of Fig. 2(b) and the values reported in Table 2. An isothermal treatment just before the temperature of titanate formation could be used successfully to improve the final density. The different microstructure observed after MgO addition is due to the different mechanism of titanate formation. MgO at first reacts with alumina to form $MgAl_2O_4$; afterwards, at ≈ 1200°C, the spinel is converted into a Mg-rich titanate solid solution $Al_{2(1-x)}Mg_xTi_{(1+x)}O_5$. The new phase particles act, therefore, as preferential sites for further titanate nucleation and growth, producing a fine-grained microstructure.[14]. The densification curves also indicate that titanate formation occurs at a reduced rate in comparison with pure Al_2TiO_5 and the probable mechanism is then solid-state diffusion through the product layer. The reduced size of the titanate particles explains the higher sintering rates in comparison with pure Al_2TiO_5 and, except SM specimens, the improved final density. The reason for the particular behaviour of SM is not completely understood. The limited densification (≈ 2·1 g/cm^3) of the matrix (probably due to the presence of aggregates of Al_2O_3 particles) achieved when the formation of titanate starts (≈ 1225°C) in comparison to the other series (2·5–2·8 g/cm^3) is likely to play an important role. The shape of the densification rate curve indicates a more complex behaviour of this system. The preferential product growth at the points of contact between reacting particles has been demonstrated to produce a porosity increase during reaction sintering of $ZnAl_2O_4$ by increasing the particle–particle distance.[19] The lower density

of SM, reducing the number of contact points between Al_2O_3 and TiO_2, could induce a process of that type, but further substantiations are required for a definitive conclusion.

5 Conclusions

Reactive sintering of Al_2TiO_5 and of a Al_2TiO_5–$MgTi_2O_5$ solid solution has been studied starting from different alumina powders but from the same TiO_2 powder. The application of dilatometric techniques allows the observation of different stages during titanate formation. Formation of pure Al_2TiO_5 initially occurs by a nucleation and rapid growth process and, afterwards, by the slow conversion of unreacted oxides controlled by solid-state diffusion. The level and nature of impurities present in the starting alumina determines the final microstructure controlling the number of 'easy to nucleate' sites, the purest aluminas resulting in the largest grains. The nature of alumina powder, determining a different microstructure evolution of the oxides matrix during heating, also affects the formation kinetics of Al_2TiO_5 and in particular the residual amount of unreacted oxides. The final density after sintering is mainly determined by the densification level of the Al_2O_3–TiO_2 matrix before titanate formation. The presence of MgO promotes a different final microstructure with a strong reduction of the average grain size, which can be more than one order of magnitude. The reaction leads to finer titanate particles which sinter at higher rates in comparison with pure Al_2TiO_5, but temperatures in the range 1500–1600°C are required for good densification. Since the initial number of titanate nuclei is mainly determined by the amount of added MgO, the final microstructure is less influenced by the nature of the alumina powder. Nevertheless, the densification of the matrix before titanate formation remain important; a high porosity has to be avoided, due to the detrimental effect on the final density.

References

1. Thomas, H. A. J. Stevens, R., Aluminium titanate—a literature review. Part 1: Microcracking phenomena. *Brit. Ceram. Trans. J.*, **88** (1989) 144–51.
2. Thomas, H. A. J. & Stevens, R., Aluminium titanate—a literature review. Part 2: Engineering properties and thermal stability. *Brit. Ceram. Trans. J.*, **88** (1989) 184–90.
3. Thomas, H. A. J., Stevens, R. & Gilbart, E., Effect of zirconia additions on the reaction sintering of aluminium titanate. *J. Mat. Sci.*, **26** (1991) 3613–16.
4. Parker, F. J., Al_2TiO_5–$ZrTiO_4$–ZrO_2 composites: a new family of low-thermal-expansion ceramics. *J. Am. Ceram. Soc.*, **73** (1990) 929–32.
5. Wohlfromm, H., Moya, J. S. & Peña, P., Effect of $ZrSiO_4$ and MgO addition on reaction sintering and properties of Al_2TiO_5-based materials. *J. Mat. Sci.*, **25** (1990) 3753–63.
6. Ishitsuka, M., Sato, T., Endo, T. & Shimada, M., Synthesis and thermal stability of aluminum titanate solid solutions. *J. Am. Ceram. Soc.*, **70** (1987) 69–71.
7. Tilloca, G., Thermal stabilization of aluminum titanate and properties of aluminum titanate solid solution. *J. Mat. Sci.*, **26** (1991) 2809–14.
8. Moroshima, H. *et al.*, Synthesis of aluminium titanate—mullite composite having high thermal shock resistance. *J. Mat. Sci. Lett.*, **6** (1987) 389–90.
9. Stingl, P., Heinrich, J. & Huber, J., Properties and applications of aluminum titanate components. In *Proceedings of the 2nd International Symposium on Ceramic Materials and Components for Engines*, Lübeck-Travemünde, Germany, April 1986, ed. W. Bunk & H. Hausner. DKG, Bad Honnef, 1986, pp. 369–80.
10. Freudenberg, B., Etude de la reaction à l'état solide $Al_2O_3 + TiO_2 \rightarrow Al_2TiO_5$. Observation des microstructures, PhD Thesis, 709, 1987, Ecole Polytechnique Fédérale de Lausanne, Lausanne, Switzerland.
11. Freudenberg, B. & Mocellin, A., Aluminum titanate formation by solid-state reaction of fine Al_2O_3 and TiO_2 powders. *J. Am. Ceram. Soc.*, **70** (1987) 33–8.
12. Freudenberg, B. & Mocellin, A., Aluminum titanate formation by solid-state reaction of coarse Al_2O_3 and TiO_2 powders. *J. Am. Ceram. Soc.*, **71** (1988) 22–28.
13. Kato, E., Daimon, K. & Takahashi, J., Decomposition temperature of β-Al_2TiO_5. *J. Am. Ceram. Soc.*, **63** (1980) 355–6.
14. Buscaglia, V., Nanni, P., Battilana, G., Aliprandi, G. & Carry, C.,Reaction sintering of aluminium titanate: I—the effect of MgO addition. *J. Eur. Ceram. Soc.* **13** (1994) 411–18.
15. Aliprandi, G., Battilana, G., Iso la, G. & 'Nanni, P., Sintering of Al_2TiO_5 from alumina at low α-content. In *Proceedings of 3eme Coll. Interrég. Europ. Ceram. 'CIEC 3'*, Lyon, France, May 1991. Soc. Chim. Ind., Lyon, 1991, p. 74.
16. Steiner C. J.-P., Hasselman, D. P. H. & Spriggs, R. M., Kinetics of the gamma-to-alpha alumina phase transformation. *J. Am. Ceram. Soc.*, **54** (1971) 412–13.
17. Philibert, J., Diffusion et transport de matière dans les solides. In *Les éditions de physique*, Paris, 1985, pp. 414–20.
18. Buscaglia, V., Bottino, C., Nanni, P.,Aliprandi, G. & Carry, C., The effect of MgO on the reactive sintering of Al_2TiO_5 starting from a commercial alumina. In *Proceedings of Engineering Ceramics '92*, Smolenice, Czechoslovakia, October 1992, ed. M. Haviar. Reproprint, Bratislava, 1993, pp. 192–8.
19. Anseau, M.R., Cambier, F. & Leblud, C., Some comments on ceramic solid-state reaction kinetics using results obtained on the ZnO–Al_2O_3 system. *J. Mat. Sci. Lett.*, **16** (1981) 1121–6.